Progress In Electromagnetics Research C, Vol. 39, 49–60, 2013

ENHANCEMENT OF PHASED ARRAY SIZE AND RADIATION PROPERTIES USING STAGGERED ARRAY CONFIGURATIONS

Abdelnasser A. Eldek*

Department of Computer Engineering, Jackson State University, Jackson, MS 39217, USA

Abstract—In this paper, two staggered array configurations are presented for enhancing size and radiation properties of wideband phased array systems. The proposed arrays are obtained either by rotating each element 45° or by inserting additional rows in the middle which are shifted by half the distance between elements. These two configurations allow for a smaller distance between array elements (29% less), while the actual distance between elements in the diagonal direction is kept the same. Reducing the distance between elements results in eliminating/reducing the grating lobes in a wider frequency range, which improves the array usable bandwidth. In addition, this proposed array produces better gain and maximum steering angle.

1. INTRODUCTION

Modern wireless communication systems often require wideband performance for multi-function and multi-channel operations. One of the most important components of these systems is phased array antenna because of its ability to steer the beam very fast by an appropriate inter-element phase control [1]. Ideally, phased array antenna system needs to be wideband with large scanning angle. Such system has to be composed of wideband radiation elements with stable radiation patterns of acceptable gain, low cross polarization, and high front-to-back ratio. The maximum steering angle is within the 3 dB beamwidth of the antenna co-polarized pattern; therefore wide 3 dB beamwidth is important characteristic of the array element. Researchers have done a lot of effort to design wideband elements with stable patterns and wide 3 dB beamwidth for phased arrays [2–7].

Received 26 February 2013, Accepted 9 April 2013, Scheduled 11 April 2013

* Corresponding author: Abdelnasser A. Eldek (abdelnasser.eldek@jsums.edu).

These efforts concentrated on increasing the antenna impedance bandwidth and enhancing its patterns and pattern stability. However, when using these antennas in phased arrays many challenges arise. If the distance between elements is more than half wavelength (at higher operating frequencies), grating lobes appear, which limits the array scanning capability and makes the usable bandwidth of the phased array much less than the bandwidth of the antenna. For example in [5], the antenna bandwidth is more than 100% while the usable bandwidth of the array is 71%. On the other hand, if the adjacent elements, sharing the same substrate, are too close, this increases the coupling due to the traveling waves in the substrate. High coupling may cause scan blindness and anomalies within the desired bandwidth and scan volume [8, 9]. In addition, the small distance with respect to wavelength (at low operating frequencies) results in low gain.

To overcome this problem, some researchers used pattern synthesis. They introduced intentional nulls on the element pattern at the locations of the grating lobes to be nullified [10]. In [11, 12], a single asymmetric ridge waveguide is used for linear arrays to achieve close element spacing in the scan plane and avoid grating lobes. These two techniques were applied on narrowband arrays like slotted waveguide and patch antenna arrays. A wideband linear phased array with unequal space was introduced in [13]. The patterns are synthesized so that no grating lobes arise in wideband. Genetic algorithms were used for sub-array amplitude weighting to reduce grating lobes, and presented in [14] for limited scanning only. A tapered balun was designed and introduced for broadband array with closely spaced elements [15]. This design is complex because the radiating elements and the tapered balun are perpendicular to each other (not planar).

In this paper, innovative staggered antenna array designs are proposed and studied for enhancing the radiation properties of phased arrays systems, and increasing the usable bandwidth of the array to be close to that of the antenna. The results shown in this paper are obtained from Ansoft High Frequency Structure Simulator (HFSS), which is based on Finite Element [16]. The antenna element used in this array is our wideband Double Rhombus antenna presented in [5, 7] for phased array applications. Prototype of the antenna is shown in Fig. 1(a).

2. PROPOSED ARRAY GEOMETRIES

Figure 1(b) shows a regular 2D array of Double Rhombus antennas. The antenna width is 12 mm and its bandwidth is 5.7–18 GHz (103%). The lowest possible element spacing "d" was found to be 14 mm,

which causes grating lobes to start arising after 10.7 GHz ($d > \lambda_0/2$). It was found that grating lobes became considerable after 12 GHz, which makes the usable bandwidth of the array 5.7–12 GHz (71%). To increase the array bandwidth, "d" has to be decreased, which requires antenna miniaturization that usually results in bandwidth and gain reduction.

Another solution to the element spacing problem is to use a staggered element spacing technique. The technique is useful for achieving tighter element spacing. Fig. 1(c) shows the first proposed staggered configuration (called Staggered Configuration 1), where the individual elements are rotated 45°. This would result in an array with the same pattern except that the polarization would be rotated 45° (in the direction of v). In this design, the spacing is still 14 mm but in the diagonal dimension. The horizontal and vertical dimensions would now be about 10 mm ($14/\sqrt{2}$). The horizontal and vertical grid is described by the centerlines in the figure. Since the grid spacing is now based on the tighter 10 mm spacing, the array can operate up to higher frequencies (at least 15 GHz) before grating lobes arise.

To regain the horizontal polarization (in x direction), the entire array of Configuration 1 can be rotated 45°, and furthermore the corner elements can be rearranged to regain the overall rectangular shape as shown in Fig. 1(d), which is called Staggered Configuration 2. Since the grid spacing is now based on the tighter 10 mm spacing in the u-v plane, the array can operate up to higher frequency before grating lobes arise. This design can also be described as if new rows of elements are placed in the middle between the rows of the regular array, but they are shifted by "$d/2$".

The couplings between elements in the regular and staggered arrays are shown in Fig. 2. For the regular array, where the distance

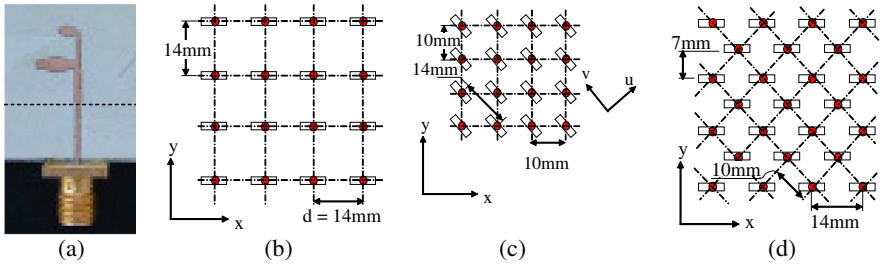

Figure 1. (a) Radiating element, and 2D array configurations: (b) regular, (c) staggered configuration 1, and (d) staggered configuration 2.

between elements is 14 mm, the average coupling is −23.4 dB. For the first staggered array configuration, the distance between elements in the u direction is 7 mm, which is the same distance for the second staggered array in the y direction. In the other directions (v and x), the distance is still 14 mm. The coupling shown in Fig. 2 for the staggered arrays is the one between elements separated by 7 mm. Although the distance is decreased to half, the coupling is still low with an average value of −20 dB. Because these two values of coupling are reasonably low, in this study we calculated the radiation patterns by multiplying the array factor by the element patterns.

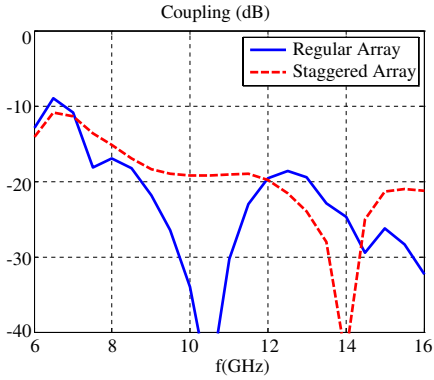

Figure 2. Coupling between elements in the (a) regular array and (b) staggered configurations.

3. RESULTS OF STAGGERED CONFIGURATIONS

Ansoft HFSS enables you to compute antenna array radiation patterns for designs that have been analyzed as single array elements. Array geometry and excitation can be defined. HFSS models the array radiation pattern by applying an array factor to the single element's patterns. Two array geometry types are supported in HFSS. The "regular uniform array" geometry defines a finite 2D array of uniformly spaced, equal-amplitude elements. The regular array type may be scanned to a user-specified direction. The regular array geometry type also allows scan specification in terms of differential phase shifts between elements. The second array is "custom array", which allows for greater flexibility. It defines an arbitrary array of identical elements distributed in 3D space with individual user-specified complex weights [16].

3.1. Staggered Configuration 1

The radiation patterns of the regular array and Staggered Configuration 1 are calculated using HFSS at different steering angles. All arrays are in the x-y plane and the steering angles are calculated from the z-axis (i.e., θ). First, the radiation patterns are calculated for a 16x16 regular array of Double Rhombus antennas, where the array size (between elements' centers) is $15 \times 14\,\text{mm} = 21\,\text{cm}$ in both axes (total area $= 21 \times 21 = 441\,\text{cm}^2$). Then, two arrays of Staggered Configuration 1 are designed and calculated. The first one has the same number of elements (16×16), which makes its size $15 \times 15\,\text{cm}^2$. The total area of this array is $225\,\text{cm}^2$ which is 49% less than regular array. The second one has the same size of the regular array, making number of elements increases to 22×22 instead of 16×16. The element is rotated 45°, then HFSS is used to calculate the patterns in the E and H planes. For this design, the E-plane is v-z and the H-plane is u-z, while in the regular array they are x-z and y-z, respectively.

Table 1 and Fig. 3 show the gain of the regular and the 2 arrays of Staggered Configuration 1. The staggered 16×16 produces almost the same gain as the regular array although it is almost half the total area. The 22×22 array provides an average gain improvement of 2.55, 2.43, and 2.4 dB in the broadside direction, 30° steering angle, and 45° steering angle, although it has the same size.

Table 1. Maximum gain.

	θ_{max}	ϕ_{max}	6GHz	8GHz	10GHz	12GHz	14GHz	16GHz
16x16	**0**	**0**	**29.7**	**29.1**	**29.9**	**30.6**	**28.7**	**29.8**
regular	**30**	**0**	**29.7**	**28.1**	**28.1**	**29**	**29.9**	**26**
array	**45**	**0**	**28.3**	**26.5**	**26.3**	**26.8**	**28.7**	**27**
16x16	**0**	**45**	**29.3**	**29**	**30**	**30.8**	**29.2**	**30.7**
Staggered	**30**	**45**	**29.6**	**28.1**	**28.1**	**29.3**	**29.6**	**26**
Config. 1	**45**	**45**	**28.4**	**26.7**	**26.4**	**27.1**	**28.6**	**26.6**
22x22	**0**	**45**	**31.6**	**31.4**	**32.3**	**33.2**	**31.6**	**33**
Staggered	**30**	**45**	**32.5**	**30.5**	**30.5**	**31.6**	**32**	**28.3**
Config. 1	**45**	**45**	**30.8**	**29.0**	**28.8**	**29.5**	**30.9**	**29**

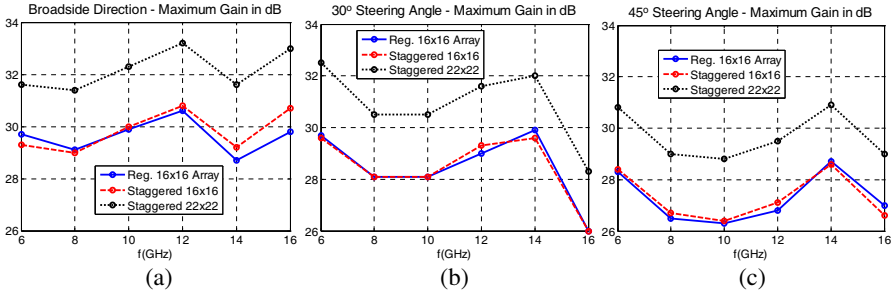

Figure 3. Maximum gain in the (a) broadside direction (0° steering angle), (b) 30° steering angle, and (c) 45° steering angle, for the 16×16 regular array, and 16×16 and 22×22 staggered array configuration 1.

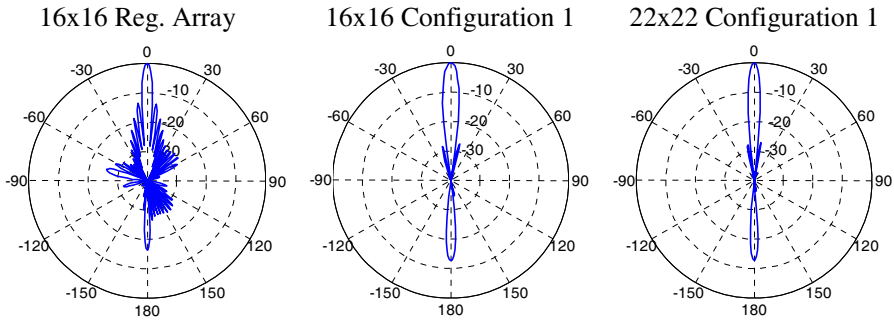

Figure 4. Radiation patterns of the regular array and staggered array configuration 1 at 16 GHz and in the broadside.

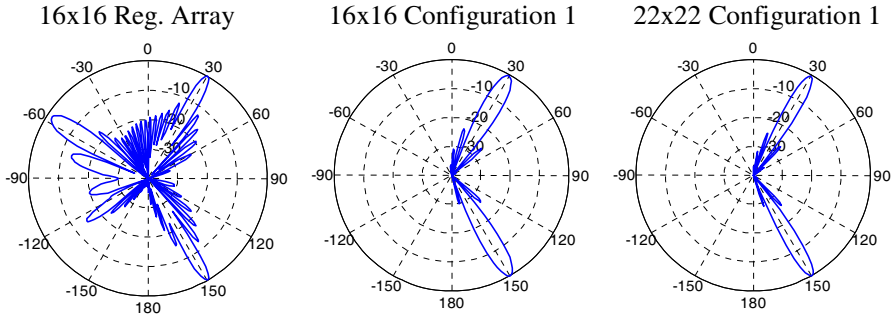

Figure 5. Radiation patterns of the regular array and staggered array configuration 1 at 16 GHz and 30° steering angle.

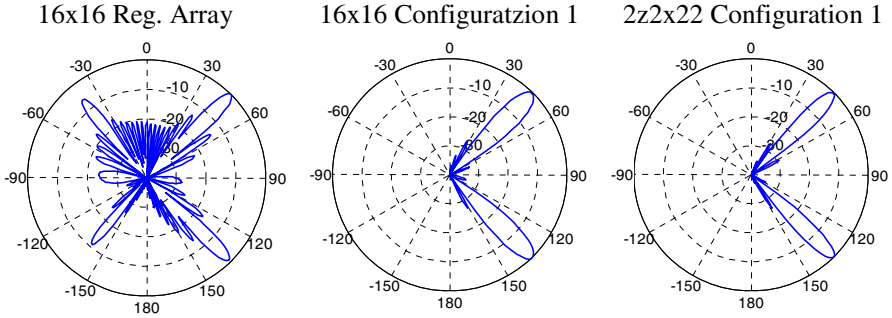

Figure 6. Radiation patterns of the regular array and staggered array configuration 1 at 16 GHz and 45° steering angle.

The radiation patterns are calculated at all frequencies, but only those at 16 GHz are shown in Figs. 4–6 to show the effect of the staggered array on the patterns and the maximum steering angle. Both staggered arrays produce nice beam with much less side lobe level. Most of the radiated power is concentrated in the main lobe which may explain the increase in the gain. For a 30° steering angle, both staggered arrays do not produce grating lobes (in the front direction of propagation between −90 and 90), while in the regular array grating lobes start arising at 14 GHz, and become very clear at 16 GHz when $\theta = -57°$ (Fig. 5). For a 45° steering angle, both staggered arrays do not produce grating lobes, while in the regular array grating lobes start arising at 14 GHz when $\theta = -56°$ and at 16 GHz when $\theta = -39°$ (Fig. 6).

After 45°, the radiation patterns of the regular array is distorted, therefore we have calculated them for the staggered arrays only, at 14 and 16 GHz. At 60° steering angle, as shown in Fig. 7, both staggered arrays produce no grating lobes and provide reasonable gain, however for a steering angle more than 60° the gain starts to reduce significantly and grating lobes start to arise in the direction of propagation ($\theta \leq |90°|$). These results show that the usable bandwidth of these staggered arrays is up to 16 GHz with a 60° maximum steering angle compared to 12 GHz with a 45° maximum steering angle in the regular array. The usable bandwidth for the staggered array is 5.7–16 GHz (95%) compared to 5.7–12 GHz (71%) for the regular array.

3.2. Staggered Configuration 2

The second array configuration is shown in Fig. 8(b). To calculate the radiation patterns of this design, special formulation is required. One

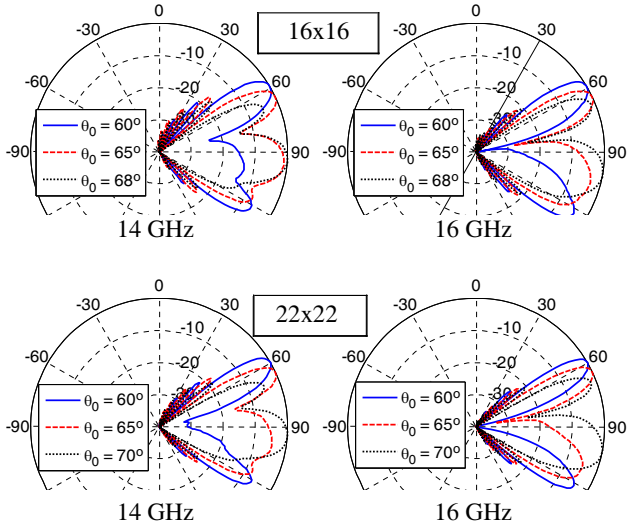

Figure 7. Radiation patterns for 16 × 16 and 22 × 22 staggered configuration 1 at 14 and 16 GHz for steering angles more than 45°.

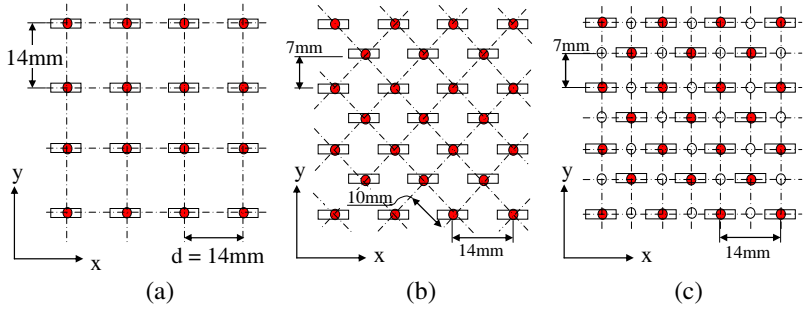

Figure 8. 2D Array configurations: (a) Regular, (b) Staggered Array Configuration 2, and (c) Modified Staggered Array Configuration 2 for radiation pattern calculation.

solution for this array is to consider it composed of two arrays: NxN array, and $(N-1)\times(N-1)$ array, where the second array has an offset of "$d/2$" in both axes, and N is the number of element per row/column in the regular array. Another solution is to add imaginary elements in the middle as shown in Fig. 8(c). The elements represented with white circles have 0V excitation, while the red circles have 1 V. This will make it equivalent to the Staggered Configuration 2, and allow us to use HFSS to calculate the radiation patterns using "custom array

Table 2. Maximum gain.

	θ_{max}	ϕ_{max}	6GHz	8GHz	10GHz	12GHz	14GHz	16GHz
16x16	**0**	**0**	**29.7**	**29.1**	**29.9**	**30.6**	**28.7**	**29.8**
regular	**30**	**0**	**29.7**	**28.1**	**28.1**	**29.0**	**29.9**	**26**
array	**45**	**0**	**28.3**	**26.5**	**26.3**	**26.8**	**28.7**	**27**
31x31	**0**	**0**	**32**	**31.7**	**32.8**	**33.5**	**32.1**	**33.2**
Staggered	**30**	**0**	**32.2**	**30.8**	**30.8**	**31.9**	**32.6**	**28.8**
Config. 2	**45**	**0**	**30.1**	**29.3**	**28.9**	**29.5**	**31.9**	**29.9**

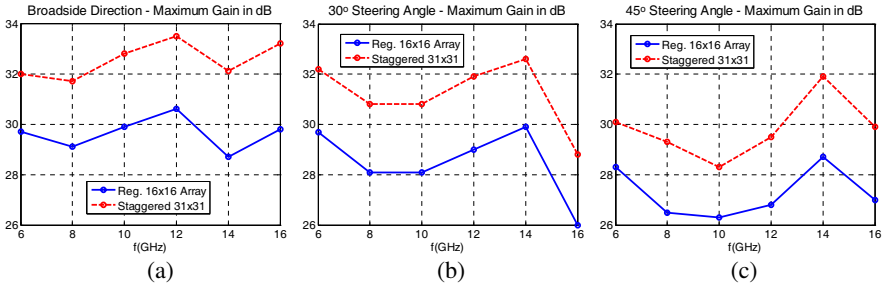

Figure 9. Maximum gain in the (a) broadside direction (0° steering angle), (b) 30° steering angle, and (c) 45° steering angle, for the 16×16 regular array, and 31×31 Staggered Array Configuration 2.

definition". To compare this array with 16×16 regular array, it has to be 31×31 with a 7 mm distance between elements to have the same size of the regular array. Matlab code was developed to define amplitudes and phases of all elements, and save them in a data file to be loaded in HFSS.

The 31×31 array is compared to the regular 16×16 array of the same size in different steering angles. Table 2 and Fig. 9 show the gain of the regular and the Staggered Configuration 2. The staggered 31×31 provides an average gain improvement of 2.92, 2.72, and 2.57 dB in the broadside direction, 30° steering angle, and 45° steering angle, without any increase in the total size.

The radiation patterns are calculated at all frequencies, but only those at 16 GHz are shown in Fig. 10 at different steering angles from

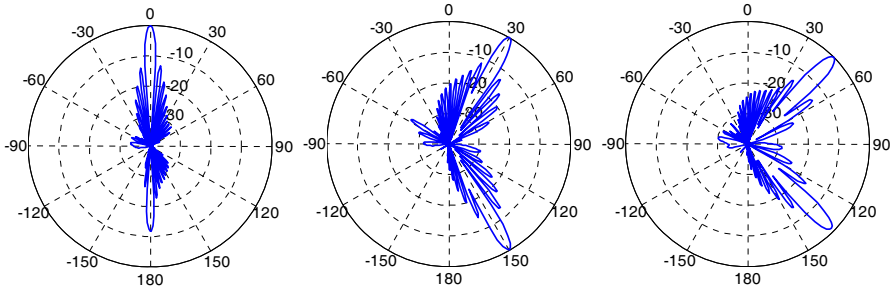

Figure 10. Radiation patterns of the staggered array configuration 2 at 16 GHz and different steering angles.

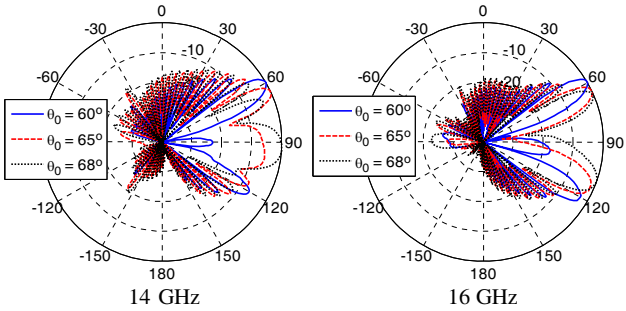

Figure 11. Radiation patterns for the 31×31 staggered configuration 2 at 14 and 16 GHz for steering angles of 60° and more.

0° to 45°. No grating lobes arise in the front direction. The back lobes will be eliminated by a ground plane. As mentioned before that after 45° the radiation patterns of the regular array is distorted, therefore we have calculated them only for this staggered array at 14 and 16 GHz. As shown in Fig. 11, acceptable pattern and gain are produced by this array at 60°. After that, the gain starts to reduce significantly and some grating lobes start to arise in the direction of propagation ($\theta \leq |90°|$). These results show that the usable bandwidth of this staggered array is similar to Configuration 1, and much better than the regular array.

4. CONCLUSIONS

Two staggered array configurations are proposed to solve the problem of grating lobes at higher operating frequencies of wideband phased array. The staggered array with the same number of elements as the

regular array (49% less in size) provides the advantages of side lobe reduction, grating lobe elimination/reduction, steering angle increase, and usable bandwidth enhancement from 71% to 95%. The staggered arrays (22×22 and 31×31) with the same size of the regular array provide the same advantages beside a 2.55 and 2.73 dB average gain enhancement. The maximum steering angle is improved to 60° at 16 GHz, instead of 45° at 12 GHz.

ACKNOWLEDGMENT

The author would like thank the Air Force Research Laboratory (AFRL) — Minority Leaders Program (MLP), and Clarkson Aerospace Corp for funding this research through contract number FA8650-05-D-1912.

REFERENCES

1. Parker, D. and D. C. Zimmermann, "Phased arrays — Part I: Theory and architectures," *IEEE Trans. Antennas Propagat.*, Vol. 50, No. 3, 678–687, Mar. 2002.
2. Eldek, A. A., "Pattern stability optimization for wideband microstrip antennas for phased arrays and power combiners," *Microwave Opt. Tech. Lett.*, Vol. 48, No. 8, 1492–1494, Aug. 2006.
3. Eldek, A. A., "Design of double dipole antenna with enhanced usable bandwidth for wideband phased array applications," *Progress In Electromagnetics Research*, Vol. 59, 1–15, 2006.
4. Eldek, A. A. and G. Zheng, "A microstrip-fed quasi-rhombus shape double dipole antenna for wideband phased array applications," *Microwave Opt. Tech. Lett.*, Vol. 48, No. 12, 2461–2464, Dec. 2006.
5. Eldek, A. A., "Ultra wideband double rhombus antenna with stable radiation patterns for phased array applications," *IEEE Trans. Antennas Propagat.*, Vol. 55, No. 1, 84–91, Jan. 2007.
6. Eldek, A. A., "Wideband 180 degree phase shifter using microstrip-CPW-microstrip transition," *Progress In Electromagnetic Research*, Vol. B, Vol. 2, 177–187, 2008.
7. Eldek, A. A., "A double rhombus antenna fed by 180 degree phase shifter for ultra wideband phased array applications," *IEEE Trans. Antennas Propagat.*, Vol. 56, No. 6, 1566–1572, Jun. 2008.
8. Chio, T. H. and D. H. Schaubert, "Parameter study and design of wideband widescan dual-polarized tapered slot antenna arrays," *IEEE Trans. Antennas Propagat.*, Vol. 48, 879-886, Jun. 2000.

9. Guo, Y. X., K. M. Luk, and K. F. Lee, "L-probe fed thick-substrate patch antenna mounted on a finite ground plane," *IEEE Trans. Antennas Propagat.*, Vol. 51, 1955–1963, Aug. 2003.
10. Shafai, L., "Scan gain enhancement in phased arrays by element pattern synthesis," *IEE Seventh International Conference on Antennas and Propagation (ICAP 91)*, Vol. 2, 914–917, 1991.
11. Shnitkin, H., J. Green, and P. J. Bertalan, "Asymmetric ridge waveguide radiating element for a scanned planar array," *IEEE Antennas and Propagation Society International Symposium*, Vol. 1, 55–58, 1988.
12. Green, J., H. Shnitkin, and P. J. Bertalan, "Asymmetric ridge waveguide radiating element for a scanned planar array," *IEEE Trans. Antennas Propagat.*, Vol. 38, No. 8, 1161–1165, 1990.
13. Song, C. and Q. Wu, "A wide-band phased array antennas with unequal space," *5th Global Symposium on Millimeter Waves (GSMM)*, 393– 96, May 2012.
14. Wang, H., D.-G. Fang, and Y. L. Chow, "Grating lobe reduction in a phased array of limited scanning," *IEEE Trans. Antennas Propagt.*, Vol. 56, No. 6, 1581–1586, 2008.
15. Xia, T., S. Yang, and Z. Nie, "Design of a tapered balun for broadband arrays with closely spaced elements," *IEEE Antennas and Wireless Propagation Letters*, Vol. 8, 1291–1294, 2009.
16. Ansoft Corporation, *HFSS: High Frequency Structure Simulator Based on the Finite Element Method*, version 14, Ansoft Corp., Canonsburg, PA, 2012.